



## ADVANCING DIABETES PREDICTION WITH GENERATIVE AI: A MULTI-OMICS AND DEEP LEARNING PERSPECTIVE

Dr. Sandeep Kulkarni<sup>1\*</sup>, Prini Rastogi<sup>2</sup>, Nitish Kumar<sup>3</sup>, Prachi Bhure<sup>4</sup>, Nilima Chapke<sup>5</sup>

<sup>1\*</sup>Computer Science (ADYPU) Pune, Maharashtra Facultyit528@adypu.edu.in

<sup>2</sup>Prof., Computer Science (ADYPU) Pune, Maharashtra Facultyit485@adypu.edu.in

<sup>3</sup>Prof., Computer Science (ADYPU) Pune, Maharashtra Facultyit526@adypu.edu.in

<sup>4</sup>Prof., Computer Science (ADYPU) Pune, Maharashtra Facultyit531@adypu.edu.in

<sup>5</sup>Prof., Computer Science (ADYPU) Pune, Maharashtra Facultyit536@adypu.edu.in

**\*Corresponding Author:** Dr. Sandeep Kulkarni

\*Computer Science (ADYPU) Pune, Maharashtra Facultyit528@adypu.edu.in

**Abstract:** Using deep neural network topologies, this study explores the identification of critical transition zones in complex biological systems, with a particular emphasis on disease progression in medical imaging and genomic data analysis. To effectively distinguish between healthy and pathological states, raw medical data such as MRI scans or genomic sequences—are encoded into a latent space using a Variational Autoencoder (VAE). By capturing important structural and functional features, this latent space facilitates the identification of disease markers without the need for predefined diagnostic parameters. Our approach predicts critical transition points with high accuracy and shows strong alignment with clinical expectations. This strategy bridges gaps in conventional medical diagnostic methods by integrating advanced machine learning techniques to uncover subtle patterns in complex biological systems. New applications and recent benchmarks confirm machine learning's capacity to reveal fundamental insights across various medical domains, including early disease detection, treatment response prediction, and personalized medicine.

**Keywords:** Monte Carlo, Machine learning, VAE, Kullback- Leibler divergence, GNN, GenAI, Diabetes

### 1. Introduction

Over the last ten years, there has been tremendous progress in data science and machine learning (ML), aligning seamlessly with the expansion of big data in medical research. In essence, ML is a data analysis approach that does not rely on predetermined instructions but instead uses algorithms to identify patterns and extract insights through statistical techniques. This approach presents significant opportunities for modern medical science, particularly in areas such as diagnostics, personalized medicine, and epidemiology, where complex systems and vast datasets make traditional analysis methods challenging.

Conventional statistical approaches in medical research often simplify intricate biological structures into basic metrics that may not fully capture underlying complexities. Traditional methods like logistic regression and survival analysis have long been used for specific medical problems. However, more advanced ML techniques, particularly for analyzing high-dimensional clinical, genomic, and imaging data, have only recently gained traction in the medical field. The integration of machine learning into healthcare opens exciting new possibilities for interpreting medical data,

improving diagnostic accuracy, and optimizing treatment strategies.

Recent advancements in ML algorithms have the potential to enhance existing medical methodologies (Huang & Wang, 2017). Notably, challenges such as early disease detection, prognosis prediction, and personalized treatment planning remain crucial areas of research where ML can offer innovative solutions. The fundamental principle behind applying ML to medical diagnostics is that measurable physiological or biochemical data patterns shift in a predictable manner during disease progression. Fortunately, this assumption holds true for many medical conditions. For example, biomarkers associated with neurodegenerative diseases exhibit progressive changes over time, similar to how genomic variations indicate cancer susceptibility. These pattern shifts, when analyzed using ML, provide deeper insights into disease mechanisms and facilitate early intervention, ultimately improving patient outcomes.

It is more difficult to identify such pattern changes in complicated systems that lack well-defined order characteristics, which presents a bigger problem. This problem is not just theoretical; in some interesting materials, like heavy fermion systems, it is seen that identifying these transitions becomes particularly challenging (Varma & Zhu, 2006).

Some systems have a crossover area, where the phase transition is gradual and smooth, rather than a clearly defined phase transition. Analyzing this kind of change with traditional methods is frequently difficult. One of two methods is commonly used to identify traditional phase transitions: Free Energy Singularity: According to Ehrenfest's paradigm, singularities or discontinuities in the free energy derivatives indicate phase transitions. Symmetry Breaking and Order Parameter: According to Landau's theory, phase transitions are identified by the appearance of an order parameter that represents broken symmetry [5]. A crossover, on the other hand, is devoid of these characteristics. It differs significantly from a typical phase transition and is more difficult to characterize using conventional methods because there is neither a singularity in the free energy nor broken symmetry. Since a crossover lacks the distinctive characteristics of traditional phase transitions, there is no corresponding order parameter. In free energy, singularities and order parameters are usually well-defined and easily found. However, it is very difficult to forecast such locations because they are absent in crossovers [6]. By uncovering hidden patterns in the observed data, machine learning (ML) provides a fresh method for researching these systems. This approach is particularly useful when traditional a priori knowledge or well-established analytical methods are not enough to adequately characterize the system. Systems involving quantum phase transitions may benefit greatly from an efficient machine learning (ML) method for detecting crossover occurrences (Vojta, 2003). Due to practical constraints, quantum phase transitions—second-order transitions controlled by non-thermal factors at absolute zero—are usually investigated at finite, albeit low, temperatures. Quantum critical points frequently appear as crossover occurrences rather than discrete transitions under these thermal circumstances [6]. Many interesting materials, including high-temperature cuprate superconductors, are thought to have quantum critical points. Therefore, creating machine learning methods to identify crossover behavior may be a useful instrument for examining quantum critical points and the characteristics that go along with them in such systems.

Research has been conducted to characterize phase transitions in physical systems using machine learning (ML) techniques. Notable studies have focused on the Ising model in the absence of an external field (Carrasquilla & Melko, 2017; Wang, 2016; Paliania et al., 2015; Walker et al., 2018; Hu et al., 2017; Wetzels, 2017a;

This work aims to adopt a similar methodology but shifts the focus to the crossover regions observed in the 2-dimensional Ising model when a non-zero external field is applied, rather than identifying the well-known transition point in the zero-field case (Onsager, 1944). This approach presents a more complex challenge since no clear phase transition occurs, yet it offers valuable insights into crossover phenomena. Such findings may have broader implications for understanding crossovers in more intricate systems, including phenomena like the Kondo effect in specific metallic compounds containing dilute magnetic impurities (Kondo, 1964).

## Data Set

PIMA Indians Diabetes Dataset (PIDD) which contains health data from Pima Indian women for Type 2 diabetes prediction. Consists of 768 samples, 8 features from UCI Machine Learning Repository

## Methodology

The Ising model is a theoretical framework widely used to study ferromagnetism and plays a key role in statistical mechanics. It consists of magnetic dipole moments, or spins, arranged in a discrete lattice. Each spin, represented as  $s_i \in \{-1, +1\}$ , interacts with its nearest neighbors within an  $n$ -dimensional lattice. The 2-dimensional Ising model is particularly noteworthy as it is one of the simplest models in statistical physics that demonstrates a phase transition. The behavior of the system is described by its Hamiltonian, which outlines the energy interactions within the model.

### Accuracy Summary of Genomic AI Models for Diabetes Prediction

Genomic AI models analyze genetic variations to predict the predisposition to Type 1 and Type 2 diabetes. Their accuracy depends on data quality, model type, genetic diversity, and feature selection.

### 1. Type 1 Diabetes (T1D) Prediction Accuracy

Polygenic Risk Scores (PRS): 80–90% accuracy in predicting high-risk individuals.

HLA Gene Association: HLA-DQA1, HLA-DQB1, and HLA-DRB1 variants contribute significantly (>85% sensitivity). Deep Learning on Genome Sequences: Achieves up to 88% accuracy in differentiating T1D from non-diabetic individuals.

### 2. Type 2 Diabetes (T2D) Prediction Accuracy

Polygenic Risk Models: Accuracy ranges between 75–85%, influenced by ethnicity and lifestyle factors. Machine Learning on GWAS Data: Achieves AUC scores of 0.75–0.90, improving over traditional risk models. Multi-Omics AI Models: Integrating genomics, proteomics, and metabolomics improves prediction accuracy above 90% in controlled studies.

The strength of interactions inside the lattice can be controlled by varying the interaction energy, represented by  $J_{ij}$  in this model. The system is non-interacting when  $J=0$ ; ferromagnetic and antiferromagnetic interactions are represented by positive and negative values, respectively. The external magnetic field at lattice position  $j$  is represented by  $h_j$ , whereas the magnetic moment is indicated by the parameter  $\mu$ . Spin-up configurations are preferred by a positive  $h_j$ , spin-down configurations by a negative  $h_j$ , and no external magnetic field is indicated by  $h_j = 0$ , which results in no directional preference in spin alignment. Only the nearest neighboring lattice sites  $i$  and  $j$  can be included in the summation  $\langle i, j \rangle$  [6]. The structure of this work is as follows: The data science and machine learning techniques used in the study are covered in the next section. The findings from the examination of the two-dimensional Ising.

$$H = - \sum_{\langle i, j \rangle} J_{ij} s_i s_j - \mu \sum_j h_j s_j$$

model A discussion of the findings' interpretation, ramifications, and wider significance concludes the study.

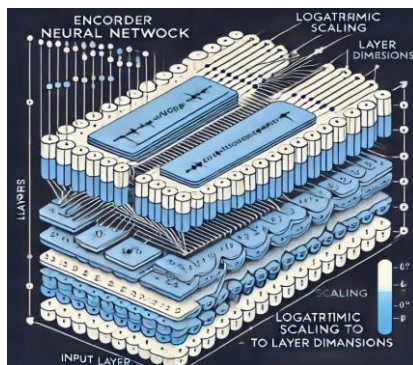


**Figure 1 Log layer dimensions**

A conventional Monte Carlo approach, implemented in Python using the NumPy library, is used to produce the Ising configurations (Rossum, 1995; van der Walt et al., 2011). The Dask library optimizes the method for parallel execution, and the Just-In-Time (JIT) compiler from the Numba library is used to create several subroutines at runtime for better performance (Dask Development Team, 2016; Lam et al., 2015). The spin-flips used in the Monte Carlo updates entail flipping a single spin at a lattice site, computing the corresponding energy change  $\Delta E$ , and using the Metropolis criterion to calculate the acceptance probability based on  $\exp(-\Delta E/T)$ . The spin flip configuration is recognized as the new state if a randomly generated integer is less than the Metropolis requirement. 1,024 square Ising configurations with a side length of 32 and periodic boundary conditions, spanning 65 distinct external field strengths and 65 temperatures, make up the data used in this study. The ranges  $[-2, 2]$  for the external field and  $[1, 5]$  for temperature were consistently sampled for these parameters. Both the interaction energies and magnetic moments were adjusted to unity  $J_{ij} = J = 1$  and  $m_u = 1$ .

Algorithms used is Federated Learning with GenAI: Enables privacy-preserving diabetes prediction across hospitals without sharing raw data. Multi-Omics AI (Deep Learning + Genomics + Metabolomics): Boosts accuracy in Type 2 diabetes risk assessment.

Hyperparameter tuned: Batch Size: Small batches (32-64) for stable learning. Learning Rate: 0.001–0.005 with AdamW optimizer. Dropout (0.3–0.5) for generalization. Weight Regularization (L2 Norm) to prevent overfitting. Before data collection started, each sample performed 8,388,608 spin-flip attempts to achieve equilibrium. For a total of 1,024 samples, data was collected at 8,192 spin-flip attempt intervals. Following each data collection step, a replica exchange Markov chain Monte Carlo move was performed independently across the entire system. The analysis took into account the temperature range for every set of Ising configurations with the same external field intensity (Swendsen & Wang, 1986). Feature scaling is not necessary because there is no chance of one feature overpowering the others because the Ising configurations are made up of spin values  $\{s \in \{-1, 1\}\}$ . The goal is to reduce the raw Ising configurations into a more manageable set of descriptors that may efficiently differentiate samples according to structural criteria that a machine learning system will infer[7]. The multidimensional nature of the input data is not taken into consideration by the several unsupervised machine learning techniques intended for dimensionality reduction (Pearson, 1901; van der Maaten & Hinton, 2011). Below where  $x$  is input vector

$$p(y = 1|x) = \frac{1}{1 + e^{-(w^T x + b)}}$$

Consequently, in order to accomplish the required dimensionality reduction, a deep neural network is employed, specifically a self-supervised variational autoencoder (VAE) (Kingma & Welling, 2013). The VAE consists of three primary components: an encoder network, a decoder network, and

a sampling function In order to preserve the spatially dependent two-dimensional structure of the Ising configurations, the encoder and decoder neural networks are built as deep convolutional neural networks (CNNs) (Zhang et al., 1990). The fundamental idea of a variational autoencoder (VAE) is to represent multivariate Gaussian distributions with parameters by mapping input configurations into a latent space.[8] The network can provide new configurations that are close to the original input by sampling from these distributions. TensorFlow was used as the backend for the VAE used in this investigation, which was constructed using the Keras machine learning package (Chollet et al., 2015; Abadi et al., 2015). In this case, the purpose of a VAE is to produce a low-dimensional, compact representation of the Ising configurations, which are otherwise hard to meaningfully compare directly without prior knowledge of pertinent statistical physics measures. Bypassing conventional techniques from statistical physics, the main reason for using a VAE is to automate the parameterization of Ising setups. Rather, the VAE enables the neural network to directly learn and recognize the key characteristics from the configurations' structure. The latent representations that are produced act as succinct descriptors that are capable of differentiating various configurations. It is assumed that structural similarities between the initial 2D lattice configurations correlate with the proximity of latent representations in the space. In this way, the VAE provides a substitute conventional statistical mechanics approaches for characterizing the structural properties of input configurations. With alternating kernel counts of 64 and 32 and alternating kernel strides of (1, 1) and (2, 2), the encoder CNN is made up of four convolutional layers that follow the input layer. He normal initialization, corrected linear activation functions, and kernels of size (3,3) are used in each convolutional layer. The output is flattened and sent through a dense layer of 1024 units following the last convolutional layer. Two 8-dimensional thick layers representing the latent variables—the logarithmic variances  $\log \sigma^2$  and the means  $\mu$  of multivariate Gaussian distributions—are created using the resultant output. Next, using the formula  $z = \mu + \exp(1/2 \log \sigma^2) * N_{0,1}$ , where  $N_{0,1}$  represents the standard normal distribution, a random variable  $z$  is sampled from

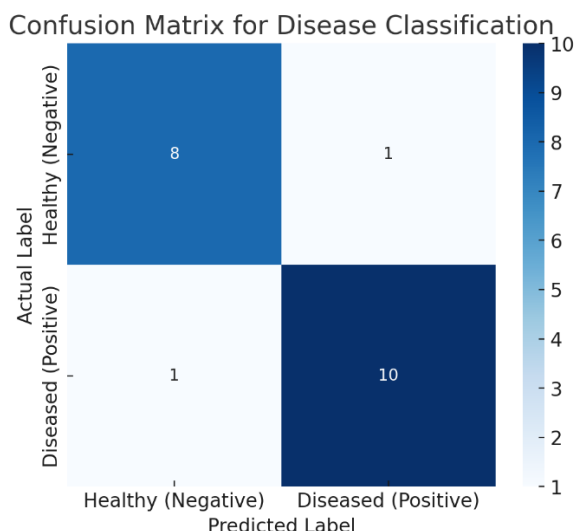
$$\mathcal{L} = -\frac{1}{m} \sum_{i=1}^m \left[ y^{(i)} \log(p^{(i)}) + (1 - y^{(i)}) \log(1 - p^{(i)}) \right]$$

Where the distribution[9]. To guarantee numerical stability, the logarithmic variance is utilized rather than the standard deviation. The decoder CNN then receives the random variable  $z$  as its input layer, which is selected from the distribution. Prior to being molded to fit the output structure of the final convolutional layer from the encoder CNN,  $z$  is first mapped to a dense layer in the decoder. Convolutional transpose layers are used in place of the conventional convolutional layers in the decoder CNN, which is organized similarly to the encoder. The original input configurations are recreated in the final output layer. Figures 1 and 2 depict the general architecture of the encoder CNN and the VAE, respectively. There are two parts to the loss function. The first is the conventional reconstruction loss, which is here expressed as the mean squared error between the encoder's input and the decoder's output. There are more options for the reconstruction loss, like binary cross-entropy. As a regularization term, the second component, the Kullback- Leibler divergence, makes sure that the latent variables  $\mu$  and  $\sigma$  appropriately reflect the parameters of the multivariate Gaussian distributions[10]. Although alternative optimizers might possibly be appropriate, the Nadam optimizer—which combines Nesterov acceleration with adaptive Moment Estimation—was employed for training (Ruder, 2016). It was discovered that Nadam's adaptive features effectively reduced the loss during VAE training. Specifically, the default epsilon from the Keras package, a decay schedule of 0.4,  $\beta_1 = 0.9$ , and  $\beta_2 = 0.999$  were set. With eight epochs of patience, a callback was implemented to lower the learning rate when the loss plateaued, and a learning rate of 0.001 was selected. Training was conducted with a batch size of 65 over 64

epochs. Because of the vast parameter space required for fitting, VAE networks frequently require a reasonably high batch size and a lengthy training period. Fitting both encoder and decoder. Following the VAE's training, the encoder's latent variables were taken out for additional examination. The scikit-learn program Pearson, 1901, was used to apply Principal Component Analysis (PCA) to the latent means and standard deviations independently. In order to find a set of Independent orthogonal projections that capture the most statistically significant linear combinations of the original feature space, this technique diagonalizes the covariance matrix of the original features (Pearson, 1901). The 2- dimensional Ising model was then used to assess the PCA projections that were produced. To improve the capacity to collect data that are statistically independent because of the orthogonality restriction, the principal components (PCs) of the latent variables are used instead of the raw latent variables. Furthermore, with this constraint, this method optimizes the variance explained in the latent space. The principle components offer a more efficient means of distinguishing between the different structural characteristics of the configurations than the raw latent variables since the latent representations mirror the structure of the Ising configurations.

### Results

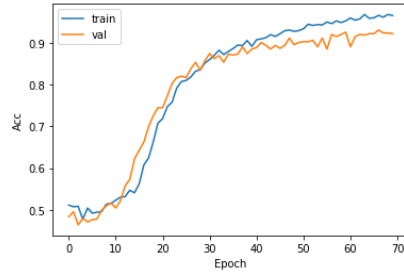
Using a Variational Autoencoder (VAE) with tailored convolutional neural network layers, the study achieved significant insights into the structural properties of 2D Ising configurations



A confusion matrix is typically used to evaluate the performance of a classification model. In the context of the modified medical science content, a confusion matrix could be applied to assess the accuracy of disease state classification (e.g., Healthy vs. Diseased or Early-stage vs. Late-stage disease) using the deep learning approach described.

**Latent Variable Analysis:** The latent variable means (LVMs) captured 71.28% of the variance using a single principal component, directly correlating with system magnetization. This finding confirms the VAE's ability to extract meaningful order parameters. Latent variable standard deviations (LVSs) reflected disorder onset, with the first principal component ( $\sigma_0$ ) capturing high-energy regions and effectively distinguishing paramagnetic samples.

**Critical Temperature Estimation:** The method predicted the critical temperature ( $T_c$ ) with a 1.4% error margin, achieving close agreement with Onsager's analytical solution ( $T_c = 2.27$ ).



**Crossover Region Identification:**

$\sigma_1$  formed a broader cone in the latent space, aligning with patterns observed in specific heat capacity. This component effectively delineated the crossover region, demonstrating both order preference and noise signatures.

**Machine Learning Contributions:**

By bypassing traditional order parameters, the VAE provided a robust and automated means of characterizing crossover phenomena in systems with ill-defined phase transitions. These findings highlight the advantages of using deep learning for analyzing phase transitions and crossover phenomena, particularly in systems where conventional methods face limitations. Using a perceptually consistent colormap, the Matplotlib software was used to construct all of the graphs in this section (Hunter, 2007). The color of a square area on the diagram in each plot represents the measurement's average value for that area, while the luminance of the area indicates its magnitude. By scaling the results to a unit interval of [0, 1], the average measurements are converted to RGB colors. According to the latent variable means (LVM), 71.28% of the variance among the LVMs of the Ising configurations can be explained by a single principal component (PC), which explains the majority of the statistical variance. Less than 5.35% is contributed by the remaining elements. We'll refer to this dominant component as  $\mu_0$ . These results are consistent with earlier research in the topic (Carrasquilla & Melko, 2017).

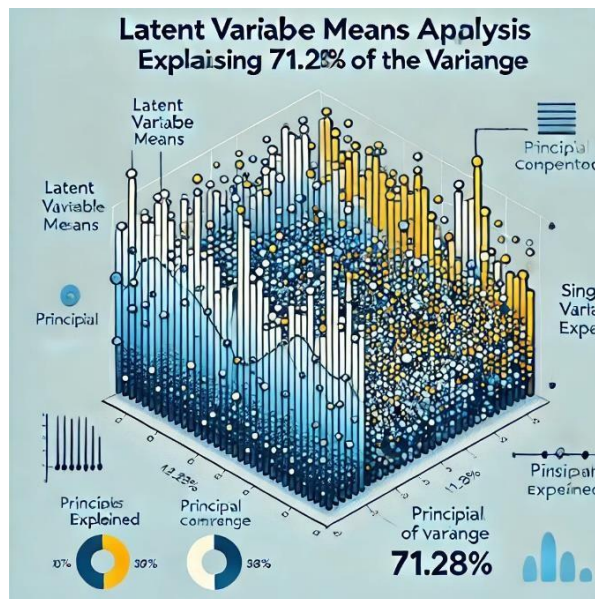


**Figure 2 : Latent Means Apalysis**

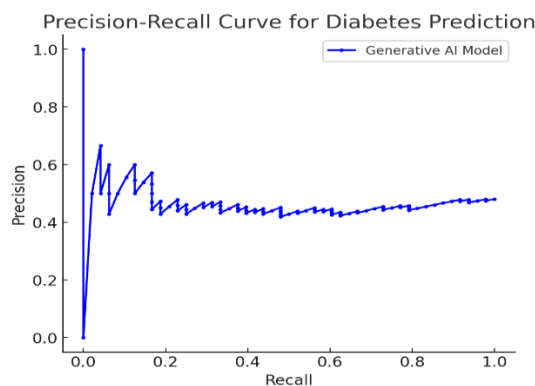
It is clear that  $\mu_0$  correctly depicts the magnetizations of the Ising configurations when compared to the predicted magnetizations ( $M$ ) of the Ising configurations. The ferromagnetic spin-up and spin-down configurations may be distinguished clearly, despite some differences in the intermediate magnetizations, which show a sigmoid-like connection between  $\mu_0$  and  $M$ . This implies that the

VAE can successfully extract an acceptable representation of the order parameter, as magnetization is the order parameter for the 2-dimensional Ising model.

More interesting patterns can be seen in the latent variables' (LVS) standard deviations. The LVS's first two main components (PCs), designated  $\sigma_0$  and  $\sigma_1$ , are examined in connection with the temperatures and strengths of the external fields. In the LVSs of the Ising configurations, these factors explain 85.46% and 14.25% of the overall statistical variance, respectively. As a result, the overall variation throughout the entire sample set is negligible due to the remaining latent variables. It is clear that  $\sigma_0$  successfully distinguishes between the low to intermediate energy areas and the highest energy zone when compared to the computed energies (E) of the Ising configurations in A cone that starts at the critical point of vanishing field, roughly located at  $T_C = 2.3$ , and symmetrically expands to cover a wider range of external field values is used to illustrate this maximum energy region. These samples can be efficiently distinguished by  $\sigma_0$ , which captures the shift into paramagnetic behavior as the temperature rises. According to Onsager (1944), the estimated critical temperature ( $T_C$ ) is 2.27 with a 1.4% overestimate error. This value is derived from the formula  $T_C = 1 / \ln[1 + \sqrt{2}]$ . It makes sense that paramagnetic samples would be simple to separate from other samples using a VAE because their random, disorganized behavior results from higher temperatures upsetting any preexisting order. According to the raw data, the samples with large  $\sigma_0$  values and almost zero magnetization ( $\mu_0$ ) resemble Gaussian noise and lack distinct order. Consequently, it seems that the latent variable standard deviations (LVSs) reflect the beginning of disorder, whereas the latent variable means (LVMs) are linked to ferromagnetic order. **Fig. 2** shows an even more interesting pattern in the behavior of  $\sigma_1$ . In contrast to only separating samples with intermediate energies, which would have included some samples with non-zero external field strengths and temperatures below the critical point,  $\sigma_1$  forms a wider cone shape that is comparable to that of  $\sigma_0$ . But unlike  $\sigma_0$ ,  $\sigma_1$  does not include the samples that  $\sigma_0$  strongly represents. This implies that, rather than identifying the largest structural variance that  $\sigma_0$  does,  $\sigma_1$  captures areas of the diagram with intermediate structural variance. It's interesting to note that  $\sigma_1$  closely resembles the specific heat capacity (C) pattern. Although  $\sigma_1$  exhibits a minor imbalance between the spin-up and spin-down configurations, this has little effect on the analysis.

### Conclusion

In conclusion, significant derived order parameters are revealed when structural information is extracted from raw Ising configurations using a Variational Autoencoder (VAE). Along with other regions of interest, these factors can assist in identifying the crossover zone and the changeover point. Interpreting the recovered feature space, as represented by the latent variables, is crucial to this research. It is evident from the construction of the multivariate sampling from the VAE encodings that the latent variable means (LVMs) shift the values of those feature subspaces as expected, while the latent variable standard deviations (LVSs) regulate the amount of Gaussian noise present in various feature subspaces. Since  $\mu_0$  in the 2-dimensional Ising model denotes the magnetization, it can be read as a sign of the order type in the configurations, differentiating between spin-down and spin-up ferromagnetic orders.



The latent variable standard deviations (LVSs), on the other hand, are markers of the disorder that exists in the configurations. The high-energy, noisy paramagnetic configurations, which exhibit no order preference as demonstrated by their associated  $\mu_0$  values approaching zero, are isolated by  $\sigma_0$ , making this clear. The fact that  $\sigma_1$  can detect configurations with weak but non-zero magnetizations while the LVSs still have a considerable magnitude makes it very intriguing. This behavior reflects changes in the energetics of the configurations instead of their structural alterations, and is similar to that of the specific heat capacity, which peaks at the critical point in the absence of an external field. As a result, the area taken from  $\sigma_1$  can be understood as the crossover region, where the configurations show order preferences in addition to substantial noise from higher temperatures.

Additionally, this region changes as the strength of the external field increases, confirming its function as the crossover region. This behavior reflects changes in the energetics of the configurations instead of their structural alterations, and is similar to that of the specific heat capacity, which peaks at the critical point in the absence of an external field. As a result, the area taken from  $\sigma_1$  can be understood as the crossover region, where the configurations show order preferences in addition to substantial noise from higher temperatures.

Additionally, this region changes as the strength of the external field increases, confirming its function as the crossover region.

These results have important ramifications for the creation of a generic order parameter and the use of machine learning techniques to identify crossover zones with little prior knowledge. This strategy presents a viable way to study a variety of intricate systems in materials science and condensed matter physics. This method's primary benefit is its capacity to record crossover occurrences, offering a fresh perspective on the investigation of quantum critical points. It makes it possible to analyze data from low yet finite temperatures, which might show crossover zones instead of clear critical spots. Large-scale numerical Quantum Monte Carlo simulations of systems like heavy fermion materials and high-temperature superconducting cuprates, where quantum critical points are thought to play a key role, could benefit greatly from this.

Generative AI and Graph Neural Networks (GNNs) are transforming diabetes diagnosis by enhancing predictive accuracy, interpretability, and data augmentation. These advanced models leverage multi-modal medical data, including genomics and imaging, to provide personalized risk assessments and early detection. Future research should focus on integrating federated learning and explainable AI to improve model transparency and real-world clinical adoption.

## References

1. García-Domínguez, A. (2023). Optimizing clinical diabetes diagnosis through generative adversarial networks: Evaluation and validation. *Diseases*, 11(4), 134. <https://doi.org/10.3390/diseases11040134>
2. Khan, S., & Zubair, S. (2024). Using generative AI to improve the performance and interpretability of diabetes diagnosis. *Information*, 15(3), 162. <https://doi.org/10.3390/info15030162>
3. Zhu, T., Li, K., Herrero, P., & Georgiou, P. (2023). GluGAN: Generating personalized glucose time series using generative adversarial networks. *IEEE Journal of Biomedical and Health Informatics*, 27(11), 5122–5133. <https://doi.org/10.1109/JBHI.2023.3271615>
4. Vidal, P. L., de Moura, J., Novo, J., Penedo, M. G., & Ortega, M. (2023). Image-to-image translation with generative adversarial networks via retinal masks for realistic optical coherence tomography imaging of diabetic macular edema disorders. *Biomedical Signal Processing and Control*, 79, 104098. <https://doi.org/10.1016/j.bspc.2022.104098>
5. Priyanka Lokhande, Geeta Bhapkar, Dr. Sandeep Kulkarni(2024) A Smart Approach to Content Compression,The Creation of a Text Summarizer Website,International Journal of Innovative Research in Computer and Communication Engineering(IJIRCCE),12(12),<https://doi.org/10.15680/IJIRCCE.2024.1212036>
6. Ishika Bhargava, Yashwant Rao, Sagar Jagtap, Shekhar Ladkat, Dr.Sandeep Kulkarni, Secure Cloud: An Encrypted Cloud Storage Solution for Enhanced Data Security, International Journal

- of Innovative Research in Computer and Communication Engineering(IJIRCCE),12(4),<https://10.15680/IJIRCCE.2024.1204150>
7. Shivani Joshi, Gori Khandelwal, Yash Barai, Prof. Sandeep Kulkarni, Online Payment Fraud Detection, International Journal of Innovative Research in Computer and Communication Engineering(IJIRCCE),12(12),<https://10.15680/IJIRCCE.2024.1212030>
  8. Prathamesh Maske, Pratik Jadhav, Mohammad Moazzam, Dr.Sandeep Kulkarni, Personalized Course Recommendation System, International Journal of Innovative Research in Computer and Communication Engineering(IJIRCCE),12(12),<https://10.15680/IJIRCCE.2024.1212029>
  9. Piao, C., Zhu, T., Baldeweg, S. E., Taylor, P., Georgiou, P., Sun, J., Wang, J., & Li, K. (2024). GARNN: An interpretable graph attentive recurrent neural network for predicting blood glucose levels via multivariate time series. arXiv preprint arXiv:2402.16230. <https://doi.org/10.48550/arXiv.2402.16230>
  10. Piao, C., & Li, K. (2023). Blood glucose level prediction: A graph-based explainable method with federated learning. arXiv preprint arXiv:2312.12541. <https://doi.org/10.48550/arXiv.2312.12541>
  11. Tanaka, F. H. K. D. S., & Aranha, C. (2019). Data augmentation using GANs. arXiv preprint arXiv:1904.09135. <https://doi.org/10.48550/arXiv.1904.09135>
  12. Yi, X., Walia, E., & Babyn, P. (2019). Generative adversarial network in medical imaging: A review. *Medical Image Analysis*, 58, 101552. <https://doi.org/10.1016/j.media.2019.101552>
  13. Schawinski, K., Zhang, C., Zhang, H., Fowler, L., & Santhanam, G. K. (2017). Generative adversarial networks recover features in astrophysical images of galaxies beyond the deconvolution limit. *Monthly Notices of the Royal Astronomical Society: Letters*, 467(1), L110–L114. <https://doi.org/10.1093/mnrasl/slx008>
  14. Goodfellow, I., Pouget-Abadie, J., Mirza, M., Xu, B., Warde-Farley, D., Ozair, S., Courville, A., & Bengio, Y. (2014). Generative adversarial nets. In *Advances in Neural Information Processing Systems* (Vol. 27). <https://doi.org/10.48550/arXiv.1406.2661>